JOURNAL OF SOLID STATE CHEMISTRY 98, 237–244 (1992)

Preparation, Structure, and Properties of Strontium-Doped Lanthanum Chromites: $La_{1-x}Sr_xCrO_3$

P. SUJATHA DEVI* AND M. SUBBA RAO

Department of Inorganic and Physical Chemistry, Indian Institute of Science, Bangalore 560 012, India

Received April 29, 1991; in revised form November 11, 1991

Strontium-doped lanthanum chromites, $La_{1-x}Sr_xCrO_3$, have been synthesised to investigate the effect of strontium doping on the stability and physico-chemical characteristics of the perovskite $LaCrO_3$. Both microscopic and X-ray examinations show that the materials exist as single phase perovskite structure for all compositions up to 50 mole% strontium substitution. The materials have been further characterized by infrared and electron paramagnetic resonance spectra. These materials show a good sinterability even in air at 1773 K. Electrical conductivity of these perovskites has been measured as a function of temperature. Electrical conductivity has been found to be a maximum at $x = 0.2$. The observed electrical and magnetic properties are consistent with activated polaron transport as the mechanism for electrical conduction in these materials.

Introduction

Materials with high electrical conductivity and chemical stability which can be used in corrosive environments as well as at elevated temperatures have been in great demand over the past several decades. Pure lanthanum chromite is extremely refractory (MP 2673 K), corrosion resistant, and has a high electrical conductivity. However, volatilization and possibly corrosion impose certain limitations on the use of pure $LaCrO_3$. The heterovalent alloying ability of $LaCrO_3$, where a fraction of M^{3+} ion (La^{3+} or Cr^{3+}) is substituted by an ion of different valence, has been exploited to improve the properties of $LaCrO_3$.

Much of the early literature on substituted lanthanum chromite appears to be confined to obtaining dense specimens. Substituents such as Sr, Mg, Ti, and Ca have been employed for this purpose (*1–7*).

In a perovskite such as $LaCrO_3$, the electrical properties may be altered either by substitution at the A lattice site (La-site) or the B site (Cr-site). A large body of information is available on the electrical properties of strontium-substituted lanthanum chromite, $La_{1-x}Sr_xCrO_3$, where x has been varied from 0.0 to 0.25 (*8–11*). Despite the extensive literature on strontium-substituted lanthanum chromites, a detailed and systematic investigation to delineate the stability region of the homogeneous perovskite phase in the system $La_{1-x}Sr_xCrO_3$ is still lacking. With a few exceptions (*12–14*) the studies carried out so far provide little information on the physico-chemical properties of strontium-substituted lanthanum chromites. The present study has been taken up

* To whom correspondence should be addressed.

0022-4596/92 $5.00

to exploit the citrate method for the preparation of strontium-substituted lanthanum chromites with a view to determining the stability range of the perovskite phase on Sr-substitution and physico-chemical characterization of these perovskite compositions.

Experimental Details

Preparation

Lanthanum biscitrato chromium complexes of the formula $La_{1-x}Sr_xCr(C_6H_5O_7)_2 \cdot nH_2O$, where x varied from 0 to 1, have been synthesized following the procedure for the preparation of lanthanum biscitrato chromium (III) dihydrate reported earlier (*15*). These precursor complexes were calcined in air at appropriate temperatures to obtain the corresponding substituted lanthanum chromites (III). All the reagents used were either analar or of higher purity.

Physical Methods

Electron micrographs were obtained using a Cambridge Stereoscan 150 scanning electron microscope (SEM). X-ray diffractograms (XRD) were recorded on a Philips PW 1050/70 diffractometer with a vertical goniometer, using Cu$K\alpha$ radiation and a scan rate of 2° min^{-1}. Cell dimensions were obtained from a least-squares refinement of the observed interplanar spacings. Infrared spectra (IR) were recorded on nujol mulls using a Perkin–Elmer 597 spectrometer. Electron paramagnetic resonance (EPR) spectra were recorded on a Varian X-band EPR spectrometer, Model E-109. Magnetic susceptibilities were measured using an EG and G Princeton Applied Research Vibrating Sample Magnetometer, Model 155. Differential Scanning Calorimetry (DSC) measurements were carried out using a Dupont 990 thermal analyser fitted with a 910 DSC accessory module. Densities of the sintered samples were obtained by determining the volume and mass of the samples directly by dimensional measurements and accurate weight and also by pyknometric methods. Conducting silver paint was applied to both the polished faces of sintered pellets. The resistivity was measured using a Gen Rad RLC Digibridge, at applied ac signal frequency of 1 KHz in the temperature range 300–500 K. The electrical resistivity was calculated using the equation

$$\rho = R\frac{A}{l}, \qquad (1)$$

where R is the measured resistance of a sample of thickness l and area of cross section A.

TABLE I

PHASE IDENTIFICATION OF $La_{1-x}Sr_xCrO_3$ COMPOUNDS

Nominal composition	Minimum calcination temperature (K)	Phases present
$LaCrO_3$	873	P
$La_{0.95}Sr_{0.05}CrO_3$	1023	P
$La_{0.90}Sr_{0.10}CrO_3$	1073	P
$La_{0.80}Sr_{0.20}CrO_3$	1073	P
$La_{0.75}Sr_{0.25}CrO_3$	1173	P
$La_{0.70}Sr_{0.30}CrO_3$	1223	P
$La_{0.60}Sr_{0.40}CrO_3$	1373	P
$La_{0.50}Sr_{0.50}CrO_3$	1573	P
$La_{0.40}Sr_{0.60}CrO_3$	1473	$LaCrO_3$ + $SrCrO_4$
$La_{0.30}Sr_{0.70}CrO_3$	1273	$LaCrO_3$ + $SrCrO_4$
$La_{0.20}Sr_{0.80}CrO_3$	1073	$LaCrO_3$ + $SrCrO_4$
$La_{0.10}Sr_{0.90}CrO_3$	1023	$SrCrO_4$

Results and Discussion

Structural Characterization

The compositions $La_{1-x}Sr_xCrO_3$, where x = 0 to 1, were prepared by calcining the corresponding citrate precursors in air for 6 hr, and the phases identified based on XRD results are summarized in Table I.

Unlike unsubstituted $LaCrO_3$, all the Sr-substituted materials were black in color, possibly owing to the presence of chromium in both trivalent and tetravalent states.

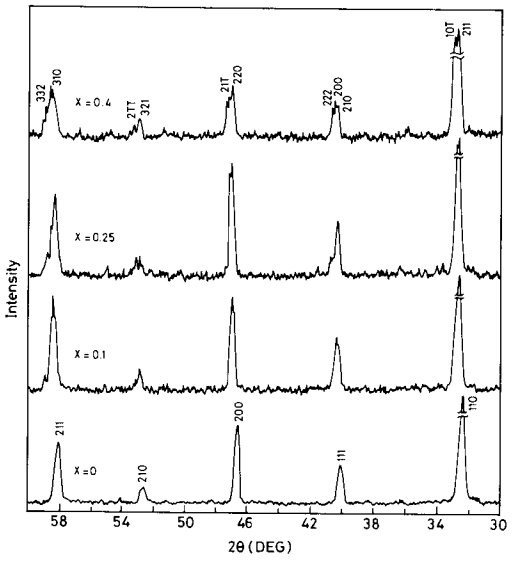

FIG. 2. Characteristic part of the X-ray diffraction showing the structural transition in $La_{1-x}Sr_xCrO_3$.

XRD pattern could be fully indexed on the basis of a rhombohedral lattice. Refined lattice parameters for the rhombohedral structure agree with the values reported by Khattak and Cox for $La_{0.75}Sr_{0.25}CrO_3$ (*14*). Relevant portions of the powder X-ray diffractograms which reveal the change of structure from orthorhombic to rhombohedral phase are shown in Fig. 2.

The phase transition orthorhombic to rhombohedral to cubic has been reported for pure $LaCrO_3$ (*16*). In order to investigate the effect of strontium substitution on the phase transition of $LaCrO_3$, differential thermograms of $LaCrO_3$, $La_{0.85}Sr_{0.15}CrO_3$, and $La_{0.65}Sr_{0.35}CrO_3$ have been recorded on a DSC in the temperature range 273–773 K. For pure $LaCrO_3$ and $La_{0.85}Sr_{0.15}CrO_3$, which are shown to be cubic by XRD, no phase transition is observed in DSC. For $La_{0.65}Sr_{0.35}CrO_3$ a transition around 588 K is indicated, which could be attributed to the rhombohedral → cubic phase transition.

Infrared Spectra of $La_{1-x}Sr_xCrO_3$

The IR spectra of a few representative Sr-substituted samples are shown in Fig. 3, along with the spectrum of pure $LaCrO_3$. With increasing Sr-substitution, a systematic shift in the Cr–O stretching (635 cm^{-1} for $LaCrO_3$) and O–Cr–O deformation (430 cm^{-1} for $LaCrO_3$) vibrations toward lower frequencies is noted. νCr–O shifts from 635 cm^{-1} for $x = 0$ to 610 cm^{-1} for $x = 0.5$. This shift possibly arises due to the changes in the force constant caused by the deformation of chromium–oxygen polyhedra. The IR spectra of compositions up to $x = 0.2$ is nearly similar to that of pure $LaCrO_3$. Beyond $x = 0.2$, significant differences are noted in the IR spectra, namely, the absence of the

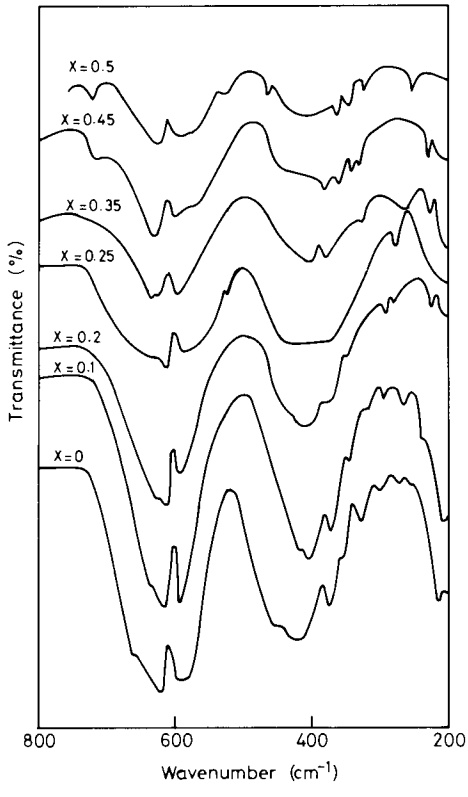

FIG. 3. IR spectra of Sr-substituted lanthanum chromites, $La_{1-x}Sr_xCrO_3$.

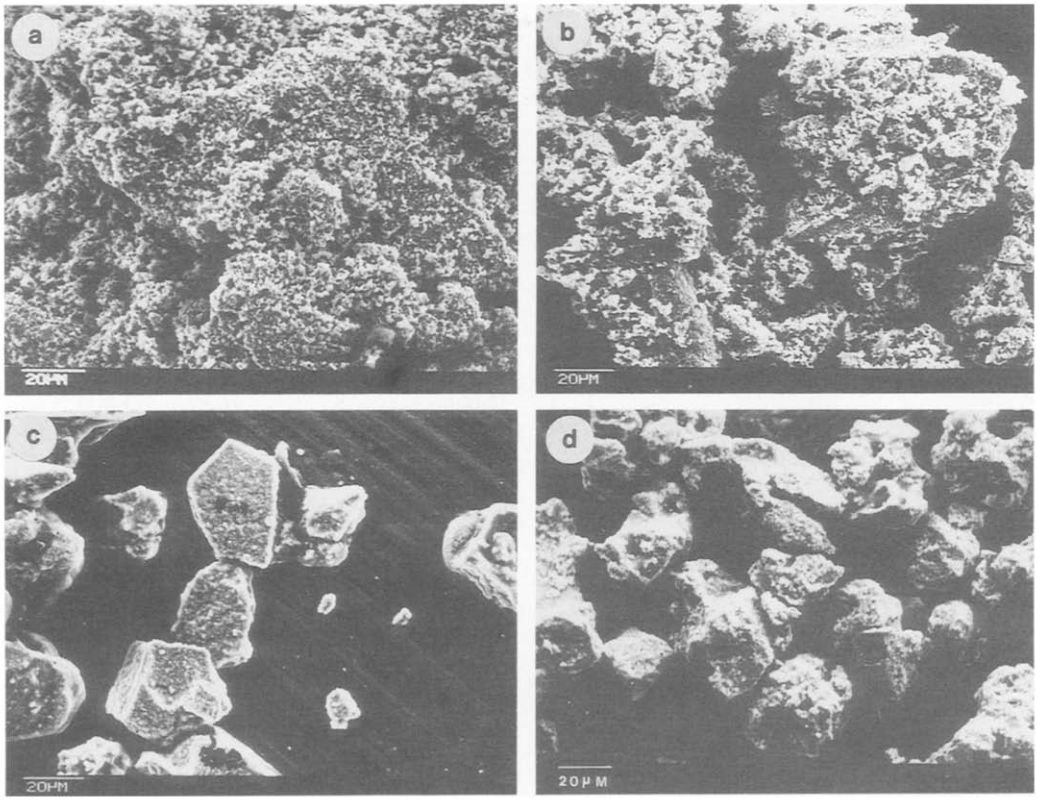

FIG. 1. Scanning electron micrographs of $La_{1-x}Sr_xCrO_3$: (a) x = 0, (b) $x = 0.25$, (c) $x = 0.45$, and (d) $x = 0.50$.

Structure and Morphology of $La_{1-x}Sr_xCrO_3$

Scanning electron micrographs (Fig. 1a–d) reveal that morphology of the strontium-substituted samples up to $x = 0.35$ is more or less similar to that of unsubstituted $LaCrO_3$. Beyond $x = 0.35$, an increase in particle size is noted and the particles also acquire a more regular geometry. This morphological change is essentially due to the increased extent of substitution of strontium.

Structural changes accompanying the substitution of La with Sr are recorded in Table II. Up to a strontium content $x = 0.2$, the pseudocubic structure of $LaCrO_3$ is retained. For $x = 0.25$ to 0.5 the powder

TABLE II

REFINED UNIT CELL PARAMETERS OF THE PEROVSKITE PHASE IN THE SYSTEM $La_{1-x}Sr_xCrO_3$

Composition	Distortion	Lattice parameters		Unit cell volume $(nm)^3$
		a (nm)	β (°)	
$LaCrO_3$	Cubic	0.3888	90.00	0.5877
$La_{0.95}Sr_{0.05}CrO_3$	Cubic	0.3879	90.00	0.5836
$La_{0.90}Sr_{0.10}CrO_3$	Cubic	0.3874	90.00	0.5814
$La_{0.85}Sr_{0.15}CrO_3$	Cubic	0.3868	90.00	0.5787
$La_{0.80}Sr_{0.20}CrO_3$	Cubic	0.3860	90.00	0.5751
$La_{0.75}Sr_{0.25}CrO_3$	Rhombohedral	0.5447	60.51	0.8262
$La_{0.60}Sr_{0.40}CrO_3$	Rhombohedral	0.5430	60.50	0.8124
$La_{0.55}Sr_{0.45}CrO_3$	Rhombohedral	0.5416	60.50	0.8124
$La_{0.50}Sr_{0.50}CrO_3$	Rhombohedral	0.5415	60.48	0.8112

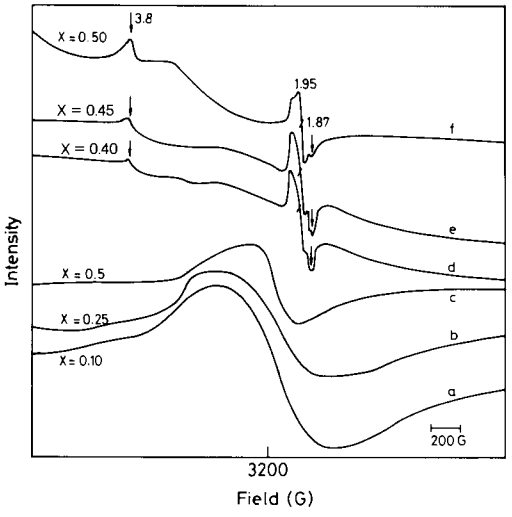

FIG. 4. EPR spectra of $La_{1-x}Sr_xCrO_3$ at 300 K (a, b, c) and at 77 K (d, e, f).

shoulder at 675 cm^{-1} (which may be assigned to a combination band of O–Cr–O bending vibrations) and broadening of the bands. These differences could be attributed to the change in the crystal structure which have been inferred from XRD.

EPR Spectra of $La_{1-x}Sr_xCrO_3$

All the Sr-substituted materials give rise to a broad EPR signal at room temperature with a g value of 1.98. For values of $x < 0.35$, EPR signals were not observed at liquid-nitrogen temperature. On increasing the Sr-concentration to $x = 0.35$, two well defined signals could be observed in the spectrum, one at $g = 1.87$ and another at 1.95. In addition, a weak signal with $g = 3.8$ is also observed (Fig. 4). The signals at 1.95 and 1.87 are due to the anisotropy probably resulting from a distortion of the "CrO_6" octahedra. The IR data is also indicative of this structural distortion.

The intensity of the signal at $g = 3.8$ though small was found to increase clearly with increase in the Sr-substitution. This signal can be attributed to a Cr^{3+}–V_O defect center similar to the defect center Fe^{3+}–V_O observed in Fe^{3+}-doped $PbTiO_3$ at $g = 5.985$ (*17*). It has been reported (*11*) that at higher Sr-substitution, the charge compensation is mainly through the formation of oxygen vacancies V_O in $La_{1-x}Sr_xCrO_3$. Our observation based on EPR study is also consistent with the above report. A few typical EPR spectra of Sr-substituted $LaCrO_3$ at 300 K are shown in Fig. 4 along with those at 77 K.

EPR spectra of one of the substituted samples, $La_{0.8}Sr_{0.2}CrO_3$ was recorded at various temperatures from 77 K upward. While the samples gave no EPR signal at 77 K, they showed signals at and beyond 133 K. For the unsubstituted sample it may be recalled that EPR signals could be observed at and above 287 K (*15*). This has been attributed to a transition from antiferromagnetic to paramagnetic state at this temperature. Thus Sr-substitution has lowered the magnetic transition temperature significantly.

Properties of $La_{1-x}Sr_xCrO_3$

Sinterability. Electrical properties of polycrystalline materials generally require sintered pellets and hence it is considered appropriate to investigate the sinterability of pure as well as substituted lanthanum chromite. Pure $LaCrO_3$ sintered in nitrogen at 1723 K for 10 hr produced pellets of only 70% theoretical density, whereas all the Sr-substituted lanthanum chromite pellets could be sintered to 85% or more of the theoretical density under the same temperature–time regions in air. We have found that doping of strontium enhanced the densification of lanthanum chromites considerably. It is pertinent here to point out that such an effect has been observed earlier by Meadowcroft in heavily Sr-doped $LaCrO_3$ (*5*).

Electrical conductivity. Figure 5 shows the temperature dependence of electrical conductivity of $La_{1-x}Sr_xCrO_3$ in a plot of

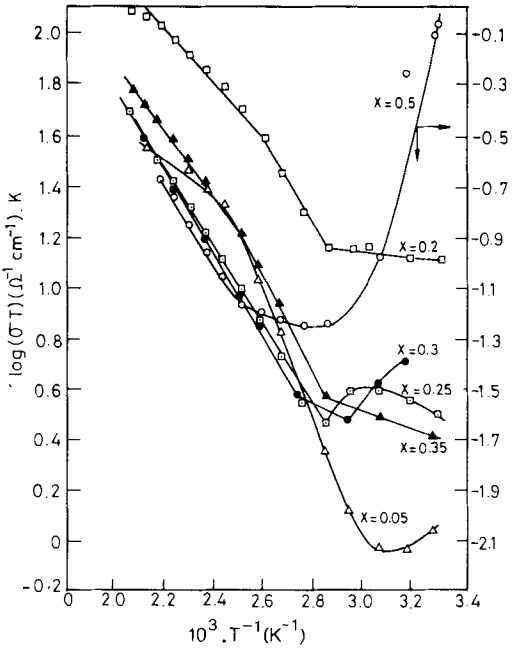

FIG. 5. Plot of log σT versus T^{-1} for $La_{1-x}Sr_xCrO_3$.

log (σT) against $1/T$. Several authors have reported that linear dependence in this plot is characteristic of the polaron hopping transport mechanism (*8, 11*). For the most part conductivity is well represented by the function

$$\sigma = \frac{1}{T}\exp\left(\frac{-Ea}{kT}\right). \qquad (2)$$

For compositions with $x = 0.05$ and 0.2, two breaks, one at 353 K and another at 413 K, are noted, similar to those observed for pure $LaCrO_3$. With an increase in Sr-substitution the activation energy for electrical conductivity is found to decrease linearly. The electrical conductivity data on Sr-substituted $LaCrO_3$ are given in Table III. At room temperature the conductivity decreases from $x = 0$ to 0.05 and then shows a linear increase with increasing Sr-content up to $x = 0.2$. Beyond $x = 0.35$ a considerable decrease in conductivity is observed. The composition with $x = 0.2$ shows the maximum conductivity among the $La_{1-x}Sr_xCrO_3$ compounds studied.

Lanthanum chromite is reported to be a *p*-type semiconductor (*8, 18, 19*), and the conductivity is essentially due to the hole motion in the *d*-electron energy levels of the chromium. When $LaCrO_3$ is acceptor doped, the dopant can be electronically accommodated by the structure in two ways:

(a) For every acceptor ion added, the transition metal ion Cr increases its oxidation state to maintain electrical neutrality. This enhances the electrical conductivity.

(b) For every acceptor ion added, to maintain electrical neutrality an oxygen vacancy occurs. This defect does not contribute to electrical conductivity. In fact conductivity will decrease in this case.

Extensive literature is available on the electrical transport properties of pure (*20–23*) as well as Sr-doped $LaCrO_3$ (*8–11*). Intrinsic conductivity in lanthanide chromites is ruled out (*20*), as it requires a much higher activation energy (1 to 2 eV) than the experimentally observed values for these compounds. It has been reported that both pure and Sr-doped $LaCrO_3$ (*8, 11*) exhibit thermally activated conductivity behavior, with doped material having a smaller activation energy for conductivity. A polaronic conduction mechanism has been suggested by a number of investigators (*8–11, 23*) for pure as well as substituted lanthanum chromites, which in turn can give rise to thermally activated conductivity.

In $La_{1-x}Sr_xCrO_3$, Sr^{2-} ions are distributed randomly on the La^{3+} lattice sites. Increases in the conductivity up to the Sr-doping level of $x \leq 0.3$ have been attributed to the formation of Cr^{4-} ions as a result of charge compensation and conduction being caused by the hopping of polarons between Cr^{3-} and Cr^{4-} ions. However, a further increase in the strontium content, i.e., x beyond 0.35, gives rise to a decrease in conductivity. For heavily doped materials, i.e.,

TABLE III

SUMMARIZED RESULTS OF ELECTRICAL CONDUCTIVITY MEASUREMENTS OF $La_{1-x}Sr_xCrO_3$ COMPOUNDS

Composition ($La_{1-x}Sr_xCrO_3$) (x)	Break temperature (K)	Activation energy (eV)	Electrical conductivity at 300 K (Ω^{-1} cm^{-1})
0.00	365	0.145 (±0.002)	8.6412×10^{-3}
0.05	328	0.182 (±0.001)	3.9570×10^{-3}
0.15			9.9824×10^{-3}
0.20	353	0.134 (±0.002)	6.3150×10^{-2}
0.25	353	0.118 (±0.003)	1.0821×10^{-2}
0.30	353	0.113 (±0.001)	9.8752×10^{-3}
0.35	341	0.127 (±0.002)	6.3143×10^{-3}
0.45	380	0.284 (±0.001)	3.6821×10^{-3}
0.50	377	0.351 (±0.001)	2.0012×10^{-3}

$x \geq 0.35$, charge compensation may take place by the creation of oxygen vacancies, which causes an effective decrease in conductivity. EPR results on these materials lend support to this change in charge compensation mechanism.

The decrease in activation energy, though very small with increasing carrier concentration, is significant and is also consistent with polaron hopping (Table III) (*24*). This is because as the polarons approach each other, their polarization clouds start to overlap and the energy required for hopping will be reduced (*25*). The activation energies for the $La_{1-x}Sr_xCrO_3$ samples though lower than those reported by Bansal *et al.* (*10*) are in agreement with those reported by Karim and Alred (*11*) and Weber *et al.* (*9*).

Magnetic Susceptibility of $La_{1-x}Sr_xCrO_3$

The effective magnetic moments of some of the Sr-substituted $LaCrO_3$ samples are given in Table IV. The paramagnetic effective moments obtained for pure $LaCrO_3$ (3.85 μ_B/Cr atom) is in good agreement with the anticipated spin only moment of 3.87 μ_B/Cr atom. If the effect of introducing Sr^{2+} ions into the lattice is to produce a corresponding number of Cr^{4+} ions, as previously postulated, we would anticipate a decrease in the effective moment with an increase in the Sr-concentration. Such an effect is born out from the data in Table IV. A similar observation has also been reported by other investigators (*10, 11*). Since our results give a clear indication of the small but systematically linear decrease in the effective moment with an increase in the Sr-concentration up to $x = 0.35$, they are consistent with the argument that the electronic transport in Sr-doped $LaCrO_3$ ($x \leq 0.3$) is associated with the presence of Cr^{4+} ions in the lattice. For compositions beyond $x = 0.35$, a slight increase in the effective magnetic moment is

TABLE IV

EFFECTIVE MAGNETIC MOMENTS AT ROOM TEMPERATURE FOR $La_{1-x}Sr_xCrO_3$

Compounds	Effective magnetic moment
$LaCrO_3$	3.85
$La_{0.95}Sr_{0.05}CrO_3$	2.85
$La_{0.90}Sr_{0.10}CrO_3$	2.41
$La_{0.85}Sr_{0.15}CrO_3$	2.27
$La_{0.80}Sr_{0.20}CrO_3$	2.11
$La_{0.75}Sr_{0.25}CrO_3$	2.04
$La_{0.70}Sr_{0.30}CrO_3$	1.93
$La_{0.60}Sr_{0.40}CrO_3$	2.07
$La_{0.55}Sr_{0.45}CrO_3$	2.10
$La_{0.50}Sr_{0.50}CrO_3$	2.36

observed, consistent with a change in the charge compensation mechanism. EPR and conductivity results also strongly support this mechanism.

Conclusions

The amorphous citrate process has been exploited to produce strontium-doped lanthanum chromite at relatively low temperature compared to the conventional ceramic methods. Both microscopic and X-ray examinations show that in the system $La_{1-x}Sr_xCrO_3$ an extensive region (up to 50 mole% strontium) occurs in which the perovskite structure exists as a single phase. A structural transition has been observed from orthorhombic to rhombohedral as a result of strontium substitution. Substitution also modifies the morphological and spectral characteristics of the perovskite $LaCrO_3$. Materials with composition up to $x = 0.30$ showed an order of magnitude increase in conductivity compared to pure $LaCrO_3$. However, a slight decrease is registered for compositions beyond $x = 0.35$. The observed conductivity and magnetic susceptibility results are consistent with the existing model proposed to explain the transport properties of $La_{1-x}Sr_xCrO_3$.

References

1. L. Groupp and H. U. Anderson, *J. Am. Ceram. Soc.* **59,** 449 (1976).
2. K. P. Bansal, S. Kumari, B. K. Das, and G. C. Jain, *Trans. J. Br. Ceram. Soc.* **80,** 215 (1981).
3. A. M. George and M. D. Karkhanawala, "Symposium on Sintering and Sintered Products," BARC, India (1979).
4. K. P. Bansal, S. Kumari, B. K. Das, and G. C. Jain, *Bull. Mater. Sci.* **3,** 435 (1981).
5. D. B. Meadowcroft, *Br. J. Appl. Phys.* **2,** 1225 (1969).
6. S. Hayashi, K. Fukaya, and H. Saito, *J. Mater. Sci. Lett.* **7,** 457 (1988).
7. N. Sakai, T. Kawada, H. Yokokawa, M. Dokiya, and T. Iwata, *J. Mater. Sci.* **25,** 4531 (1990).
8. J. B. Webb, M. Sayer, and A. Mansing, *Can. J. Phys.* **55**(19), 1725 (1977).
9. W. J. Weber, C. W. Griffin, and J. L. Bates, *J. Am. Ceram. Soc.* **70**(4), 265 (1987).
10. K. P. Bansal, S. Kumari, B. K. Das, and G. C. Jain, *J. Mater. Sci.* **18,** 2095 (1983).
11. D. P. Karim and A. T. Aldred, *Phys. Rev. B* **20**(6), 2255 (1979).
12. D. J. Anderton and F. R. Sale, *Powder Metall.* **22**(1), 14 (1979).
13. K. P. Bansal, S. Kumari, B. K. Das, and G. C. Jain, *J. Mater. Sci. Lett.* **1,** 239 (1982).
14. C. P. Khattak and D. E. Cox, *J. Appl. Crystallogr.* **10,** 405 (1977).
15. P. Sujatha Devi and M. Subba Rao, *Thermochim. Acta* **153,** 181 (1989).
16. R. Balachandran, Ph.D. thesis, p. 76, Indian Institute of Science, Bangalore (1985).
17. S. Geller and P. M. Raccah, *Phys. Rev B* **2**(4), 1167 (1970).
18. I. G. Austin and N. F. Mott, *Adv. Phys.* **18,** 41 (1969).
19. J. Jacobs, K. M. Castellizo, W. Manuel, and H. W. King, *in* "Conference on High Temperature Science Related to Open Cycle Coal Fired MHD Systems," Vols. 21–27, p. 148. Argonne National Laboratory, (1977).
20. G. V. Subba Rao, B. M. Wanklyn, and C. N. R. Rao, *J. Phys. Chem. Solids* **32,** 345 (1971).
21. A. K. Tripathi and H. B. Lal, *Mater. Res. Bull.* **15,** 233 (1980).
22. A. K. Tripathi and H. B. Lal, *J. Mater. Sci.* **17,** 1595 (1982).
23. Kanchan Gaur, S. C. Varma, and H. B. Lal, *J. Mater. Sci.* **23,** 1725 (1988).
24. N. F. Mott and E. A. Davis, "Electronic Processes in Noncrystalline Materials," Clarendon Press, Oxford (1971).
25. N. F. Mott, *J. Non-Cryst. Solids* **1,** 1 (1968).